Chemical Research in Toxicology

Article

pubs.acs.org/crt

The Butter Flavorant, Diacetyl, Exacerbates β-Amyloid Cytotoxicity

Swati S. More, Ashish P. Vartak, and Robert Vince*

Center for Drug Design, Academic Health Center, University of Minnesota, 308 Harvard Street SE, 8-123A WDH, Minneapolis, Minnesota 55455, United States

Supporting Information

ABSTRACT: Diacetyl (DA), an ubiquitous butter-flavoring agent, was found to influence several aspects of amyloid-β (Aβ) aggregation—one of the two primary pathologies associated with Alzheimer's disease. Thioflavin T fluorescence and circular dichroism spectroscopic measurements revealed that DA accelerates $Aβ^{1-42}$ aggregation into soluble and ultimately insoluble β-pleated sheet structures. DA was found to covalently bind to Arg^5 of $Aβ^{1-42}$ through proteolytic digestion–mass spectrometric experiments. These biophysical and chemical effects translated into the potentiation of $Aβ^{1-42}$ cytotoxicity by DA toward SH-SY5Y cells in culture. DA easily traversed through a MDR1-MDCK cell monolayer, an in vitro model of the blood–brain barrier. Additionally, DA was found not only to be resistant to but also inhibitory toward glyoxalase I, the primary initiator of detoxification of amyloid-promoting reactive dicarbonyl species that are generated naturally in large amounts by neuronal tissue. In light of the chronic exposure of industry workers to DA, this study raises the troubling possibility of long-term neurological toxicity mediated by DA.

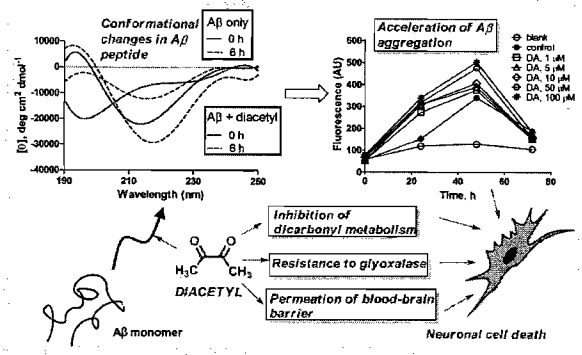

INTRODUCTION

The amyloid-β (Aβ) peptides are established mediators of Alzheimer's disease (AD) pathology. These peptides are cleavage products of the transmembrane-situated amyloid precursor protein (APP). Cleavage of APP consists of two sequential proteolytic events, the natures of which dictate the amyloidogenic (misfolding) potential of the products. Cleavage of APP by the membrane-bound α-secretase between lysine and leucine residues at the N-terminal followed in turn by intermembrane cleavage of the liberated fragment by γ-secretase releases the nonamyloidogenic $Aβ^{17-40}$ and $Aβ^{17-42}$ fragments. If the first event is mediated by β-secretase instead, the amyloidogenic fragments $Aβ^{1-40}$ and $Aβ^{1-42}$ are produced.[1,2] Amyloidogenesis includes several orders of Aβ association, yielding soluble as well as insoluble oligomers.[3] Physiological concentrations of $Aβ^{1-42}$ have been estimated to be in the range of 0.1–1 nM in the CSF.[4] Similar concentrations have been found to be mirrored in the ISF.[5] $Aβ^{1-42}$ combines with entities such as serum amyloid protein and other glycoproteins to form the plaques diagnostic of AD.[6] Each stage of Aβ elicits its deleterious effects on neuronal tissue and nerve conduction in a unique manner. For example, soluble aggregates and protofibrils participate in an increase in cellular oxidative stress, while insoluble fibrils affect cellular ion channels causing disruption of Na^+/K^+ and Ca^{2+} balance and by deposition in the synaptic clefts affecting nerve signal conduction.[7,8] While understanding of the mechanisms through which Aβ aggregates affect neuronal tissue is at best rudimentary, it is unequivocally agreed upon that Aβ aggregation is a pathogenic event.

Inception and progression of AD have been empirically linked to "oxidative stress" in neuronal tissue, which embodies pathological tilt in redox balance toward oxidative reactions. Reactive carbonyl species (RCS) such as methylglyoxal (MEG) and glyoxal are examples of metabolically produced oxidants that form covalent adducts with proteins termed advanced glycation end products (AGEs).[9] Such transformations fundamentally alter peptide or protein structure and function. Aβ peptides are subject to such modifications, the outcome of which may alter their conformation and therefore their ultimate metabolic fate. The amyloidogenic Aβ peptides equilibrate between three major conformations: random-coil, α-helix, and β-strand.[10] The former is a higher energy structure, while the latter two are local minimas. The random-coil conformation is subject to proteolytic digestion and is therefore not a progenitor of toxic aggregates. The α-helix is similarly incapable of aggregation. The β-strand structure, however, is prone to aggregation and is the conformation of interest in Aβ pathology.[11] Hydrophobic interaction of amino acid side chains provides energetic stabilization toward association of β-strands to form β-sheets. The C terminus of $Aβ^{1-42}$ (residues 20–42) is mainly hydrophobic while the N terminus (residues 1–15) is hydrophilic. Residues 16–20 constitute the crucial KLVFF motif that is essential for aggregation.[12] The strand-turn-strand motifs constituting Aβ fibrils require the hydrophilic N terminus to become desolvated.[13] The presence of hydrophilic interactions during $Aβ^{1-42}$ folding implies that covalent

Received: March 5, 2012

   dx.doi.org/10.1021/tx3001016 | Chem. Res. Toxicol. XXXX, XXX, XXX–XXX

modification of the Lys[16], Lys[29], and Arg[5] residues would affect folding dynamics. On first glance, it would seem that masking of electrostatic charge on the Lys or Arg residues through AGE production would render the peptide hydrophobic and therefore promote folding. In actuality, the net effect is different for every known AGE of Aβ. Modification of Aβ by MEG increases the percentage of β-strand structure and therefore aggregation propensity.[14] The AGE formed by a metabolite of nicotine on the other hand sterically occludes Lys[16], impeding β-sheet formation.[15]

The flavorant, diacetyl (2,3-butanedione, DA), has been the focus of a considerable amount of toxicological research because of its ability to induce bronchiolitis obliterans in popcorn factory workers upon chronic exposure.[16] The structural similarity of DA to physiologically occurring dicarbonyl species suggests that it may form AGEs. Exposure levels of DA to popcorn factory workers in the mixing area of the plant are around 32 ppm on an average but may reach a disturbingly high peak level of 1230 ppm in certain areas![17] A rather high exposure level of 525 ppm has also been recorded in the flavor manufacturing industry.[18] In light of chronic exposure of popcorn factory workers to DA and the structural similarity of DA to MEG, a known $A\beta^{1-42}$ aggregation inducer, an investigation into the amyloidogenic effects of DA is clearly warranted. In this study, we seek to answer the following specific questions: (1) Does DA influence $A\beta^{1-42}$ structural dynamics and/or aggregation; (2) does DA influence the cytotoxicity of $A\beta^{1-42}$; (3) is DA capable of traversing the barrier between the plasma and the CNS; and, finally, (4) is DA subject to detoxification by one of the major metabolic pathways for dicarbonyls such as MEG in the brain (the glyoxalase pathway).

MATERIALS AND METHODS

Drugs and Reagents. DA, MEG, thioflavin T (ThT), metformin, D-penicillamine, 2-thiobarbituric acid, and 3-(4,5-dimethylthiazol-2-yl)-2,5-diphenyltetrazolium bromide (MTT) were purchased from Sigma (St. Louis, MO). Stock solutions of all compounds (10 mmol/L) were freshly prepared in PBS for every experiment. A stock solution of the MTT reagent was prepared in PBS at 5 mg/mL concentration and was stored at 4 °C up to 2 weeks from preparation under protection from light. β-Amyloid peptide 1–42 ($A\beta^{1-42}$) was obtained from American Peptide Company (Sunnyvale, CA). For all experiments unless otherwise mentioned, $A\beta^{1-42}$ was dissolved in 100% 1,1,1,3,3,3-hexafluoro-2-propanol (HFIP) to a concentration of 1 mg/mL, sonicated in a water bath for 10 min, and dried under vacuum. The HFIP-treated $A\beta^{1-42}$ was dissolved in dimethylsulfoxide (DMSO) to a final concentration of 1 mM and stored at −20 °C.

Cell Culture. The cell culture media DMEM H-21, MEM, F12, and fetal bovine serum (FBS) were obtained from Invitrogen (Carlsbad, CA). The human neuroblastoma cell line, SH-SY-5Y, used in the present study was obtained from American Type Culture Collection (Manassas, VA). Wild-type (WT) and MDR1-transfected epithelial Madin–Darby canine kidney (MDCKII) cells were generously obtained from Prof. William Elmquist (Department of Pharmaceutics, University of Minnesota). The SH-SY-5Y cells were maintained in MEM:F12 (1:1) medium supplemented with 10% FBS, 100 units/mL penicillin, and 100 units/mL streptomycin and 1% NEAA (non-essential amino acid). The MDCK cell line was cultured in DMEM H-21 medium supplemented with 10% FBS, 100 units/mL penicillin, and 100 units/mL streptomycin. The MDR1-MDCK cell growth media additionally contained 80 ng/mL of colchicine for positive selection of P-gp expression. All of the cell lines were maintained at 37 °C in a humidified atmosphere with 5% CO_2/95% air.

ThT Assay. Rapid association of ThT with $A\beta^{1-42}$ aggregates of orders higher than dimers[19] causes the appearance of a new excitation maximum and a corresponding enhanced emission in contrast to the free dye. $A\beta^{1-42}$ (final concentration at 10 μM) was incubated in the presence and absence of DA (0–100 μM concentrations) in a total reaction mixture of 200 μL in PBS at 37 °C. Aliquots of the reaction solution (20 μL) were transferred to a black microfluor plate containing 200 μL of ThT solution at a concentration of 20 μM in 50 mM glycine–NaOH buffer (pH 8.5) at various time intervals for fluorescence readings. The fluorescence was monitored at an excitation wavelength of 440 nm and an emission wavelength of 500 nm using BioTek Synergy HT microplate reader (BioTek Instruments, Winooski, VT).

Circular Dichroism (CD) Studies. Changes in the secondary solution structure of $A\beta^{1-42}$ were determined by CD studies.[20] $A\beta^{1-42}$ was dissolved in HFIP/H_2O (1:1) and incubated at ambient temperature for 1 h. The solution was then evaporated under reduced pressure (<0.01 mmHg) to afford a film. The film was dissolved either in 2 × PBS or in a freshly prepared 25 μM solution of DA in 2 × PBS. Aliquots of these solutions were placed in sealable cuvettes (0.1 cm × 1.0 cm × 4.5 cm, Starna, Atascadero, CA), and the cuvettes were sealed. The cuvettes and the remainder of the solutions were maintained at 37 °C for the duration of the experiments. Ellipticities of the samples and corresponding photomultiplier voltages were recorded on a Jasco J-815 CD spectrophotometer between a wavelength range of 190 and 250 nm utilizing a path length of 1 cm. The Jasco Data Analysis program was utilized to subtract ellipticities of blanks (2 × PBS and 25 μM DA in 2 × PBS, respectively) from the two samples. The resulting CD spectra were analyzed by polynomial regression curve fitting as provided in the Prism program. CD spectra of aliquots from the remainder of the solutions were recorded periodically and compared with the samples to ascertain the lack of aggregation seeding or other effects from the container walls.

Mass Spectrometry. $A\beta^{1-42}$ was prepared in a manner akin to that for the CD studies. For obtainment of the ESI-MS spectrum of the adduct of DA with $A\beta^{1-42}$, the lyophilized peptide was dissolved in a 25 μM solution of DA in PBS (to a 25 μM final concentration of Aβ) and aged at 37 °C for 24 h. A 25 μL aliquot was injected into a mass spectrophotometer with an electrospray ionization source fed into a quadrupole TOF analyzer. For limited proteolytic digestion studies, the lyophilized peptide was dissolved in PBS to a final concentration of 25 μM and diluted to twice its volume by a 1 μM solution of dithiothretol. The entirety of the solution was lyophilized and dissolved in freshly constituted Glu-C lysis buffer (1 mL) containing Glu-C (20 μg).[21] After incubation for 24 h followed by freezing at −80 °C and speed drying to halt enzyme activity, the lyophilized residue was reconstituted in ultrapure water, desalted by passage through a Zip-Tip, and submitted for MALDI-TOF analysis to the University of Minnesota Center for Mass Spectrometry and Proteomics.

Cytotoxicity Studies. SH-SY-5Y cells were seeded in 96-well plates at a density of 30000 cells/well. After overnight incubation, the cells were exposed to three different conditions: (1) DA alone (50 μM), (2) $A\beta^{1-42}$ alone (10 μM), and (3) a combination of DA (50 μM) and $A\beta^{1-42}$ (10 μM) for 24 h at 37 °C. The drug-containing medium was replaced with fresh media at the end of 24 h, and the incubation was allowed to continue for an additional 24 h. At the end of the incubation, 20 μL of MTT stock solution (5 mg/mL) was added to each well and incubated for 3 h at 37 °C. The MTT reaction medium was discarded, and the purple-blue MTT formazan crystals were dissolved by the addition of 100 μL of 0.1 N HCl in isopropanol. The optical density (OD), a reflection of mitochondrial function of the viable cells, was read directly with a microplate reader (BioTek SynergyHT) at 580 nm and a reference wavelength of 680 nm. Concentration–response graphs were generated for each drug using GraphPad Prism software (GraphPad Software, Inc., San Diego, CA). Results are expressed as mean percent of cell growth with respect to control with the standard error of the mean. The same experiment was repeated with a range of DA concentrations (0–1000 μM).

Similar procedures were used for determining the protective effect of carbonyl scavengers against DA-induced increase in $A\beta^{1-42}$ cytotoxicity. In this case, DA (50 μM) was allowed to react with

dx.doi.org/10.1021/tx3001016 | Chem. Res. Toxicol. XXXX, XXX, XXX–XXX

metformin, D-penicillamine, or 2-thiobarbituric acid (1 mM) for 30 min at 37 °C before their addition to cells. A solution of β-amyloid peptide ($A\beta^{1-42}$) was then added to each well so that the resulting concentration of the peptide was 20 μM. The cells were subjected to the aforementioned conditions for 24 h at 37 °C. The media containing treatment compound solutions was then replaced with fresh media, and the cell viability was determined by the MTT assay at the end of additional 24 h as described earlier.

In Vitro Directional Transport Experiment Using MDCK Cell Monolayer. The influence of the blood–brain barrier (BBB) on the permeability of DA was determined by MDCK cell monolayers growing on a permeable support. MDCK cells, WT and MDR1 transfected, were seeded into six-well Transwell permeable supports (2.4 cm in diameter, 0.4 μm pore size; 3412, Corning Life Sciences, Lowell, MA) in growth medium at a density of 3.0×10^5 cells per well and allowed to grow to confluence for 3 days.

For the experiment, the cells were washed and preincubated with the assay buffer for 30 min. The assay buffer was then replaced with one containing DA (100 μM) in the donor side, that is, the apical side (1.5 mL), to determine flux from the apical to the basal side. Alternatively, DA-containing buffer was placed on the basal side (2.6 mL) to determine flux from the basal to the apical side. Drug-free fresh assay buffer was placed on the receiver side. The experimental wells were incubated on an orbital shaker at 37 °C for the duration of the experiment (90 min) except while drawing samples and replacing the assay buffer. One hundred microliter samples were drawn from the receiver side at 0, 5, 10, 15, 20, 30, 40, 50, 60, 75, and 90 min and replaced with drug-free fresh assay buffer. Similarly, 100 μL samples were drawn from the donor side at 0 and 90 min and replaced with the assay buffer containing DA.

All of the aliquots were analyzed by HPLC assay after derivatization with 1,2-diaminobenzene.[22] To the 100 μL of assay aliquot to be analyzed was then added 2 μL of 0.1 N NaOH to bring the pH to 8.0. This was followed by the addition of 20 μL of 1,2-diaminobenzene (10 mM) and 10 μL of internal standard, 5-methylquinoxaline (1 μM), and the total volume was adjusted with assay buffer to 150 μL. Samples were incubated at 60 °C for 3 h and then analyzed by HPLC.

Assay Buffer. NaCl (7.13 g), $NaHCO_3$ (2.10 g), glucose (1.8 g), HEPES (2.38 g), KCl (0.224 g), $MgSO_4$ (0.295 g), $CaCl_2$ (0.206 g), and K_2HPO_4 (0.070 g) in 1000 mL of H_2O adjusted to pH 7.4.

HPLC System. Beckman Coulter Gold; UV detection, 313/315 nm; column, Varian Microsorb C18, 5 μm, 4.6 mm × 250 mm; solvent system, linear gradient 20–80% solvent B [solvent A = 10 mM KH_2PO_4 (pH 2.5); solvent B = acetonitrile]; flow rate, 1.0 mL/min; retention time (t_R), DA 8.00 min; internal std., 9.00 min.

The apparent permeability (P_{app}) was calculated by the following equation:

$$P_{app} = \frac{\left(\frac{dQ}{dt}\right)}{A \times C_0}$$

where dQ/dt is the mass transport rate as obtained from the slope of the amount transported versus time plot, A is the apparent surface area of the cell monolayer (4.67 cm^2), and C_0 is the initial donor concentration. ^{14}C-Mannitol transport and transepithelial electrical resistance (TEER) were measured to validate the integrity of the MDCK cell monolayer.

Glyoxalase I (Glx-I) Enzyme Kinetics Assay. DA was examined for its ability to act as a substrate for the yeast Glx-I. The commercial 40% MEG solution was distilled to remove polymerization products as described earlier.[23] Enzymatic assays were carried out according to the conditions that we have previously described.[24] Concentrations of MEG and DA employed in this assay were 5 mM, while that of glutathione was 1 mM. An increase in absorption at 240 nm was employed as a measure of the formation of the product of the enzymatic reaction with glutathione and MEG over a period of 20 min. In lieu of information about the absorption characteristics of an incubate with DA, we scanned the 200–400 nm wavelength region.

For measuring time dependency of the inhibition of Glx-I by DA, Glx-I (1.4 μM) was combined with DA (0–1000 μM) in 0.05 M potassium phosphate buffer (pH 6.6) at 25 °C. Samples were withdrawn at various time points (0, 5, 15, 30, 45, 60, 90, 120, 150, and 180 min) and examined for residual enzyme activity as described above. The activity remnant at a given time was expressed relative to an incubate without DA.

Apparent rate constants of inactivation k_{obs} were available for each DA concentration through fitting initial velocities achieved by the enzyme preincubation mixtures at each time point to the standard exponential rate eq I

$$[P] = v_0 e^{-k_{app} t} \quad \text{(I)}$$

where P is the concentration of product formed when the enzyme is preincubated with the concentration of DA in question for an amount of time t. The maximum rate constant for inactivation, k_{inact}, and the steady-state rate constant of inactivation K_I were extracted by fitting k_{obs} and the concentration of DA, I, to eq II.

$$k_{obs} = \frac{k_{inact}}{1 + K_I/[I]} \quad \text{(II)}$$

Statistical Analysis. Data were analyzed by two-tailed unpaired t tests using Prism 5.0 software (GraphPad, San Diego, CA). $P < 0.05$ was considered statistically significant.

RESULTS

Aggregation Studies. *DA Induces Increase in $A\beta^{1-42}$ Aggregates Detectable by ThT Fluorescence.* The ThT-induced fluorescence intensity of $A\beta^{1-42}$ alone in solution rose 6-fold over a period of 48 h (Figure 1). The progression of fluorescence intensity is sigmoidal, with the lag phase being ascribed to nucleation/seeding of aggregation before rapid growth in soluble aggregate population. A decrease in intensity after 48 h denotes precipitation of aggregates.

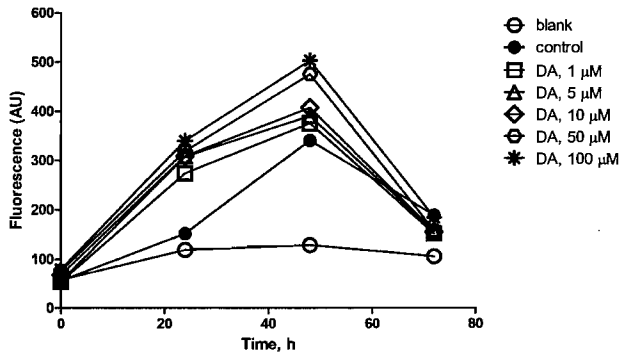

Figure 1. Effect of DA on $A\beta_{1-42}$ β-sheet formation evaluated by the ThT assay. $A\beta_{1-42}$ (10 μM) was incubated in the presence and absence of DA (0–100 μM) in PBS at 37 °C. Aliquots of the reaction solution were mixed with the ThT solution (20 μM) and analyzed as described in the Materials and Methods. Data are the results from a single experiment. Similar results were obtained in three independent experiments.

The addition of DA in concentrations corresponding to 0.1–10 mol equiv with respect to $A\beta^{1-42}$ caused a concentration-dependent increase in the rate of soluble aggregate formation. A 4.5–5.6-fold increase in fluorescence was noted at 24 h. The fluorescence at 48 h was unchanged for the subequivalent concentrations of DA and increased slightly (1.2-fold) when DA was present in 10-fold molar excess (Figure 1).

CD Studies Delineate the Structural Changes Caused by DA in $A\beta^{1-42}$. Solutions of $A\beta^{1-42}$ in PBS without pretreatment with HFIP–H_2O afforded CD curves indicating predominant β-sheet structure; however, their ellipticities deteriorated

dx.doi.org/10.1021/tx3001016 | Chem. Res. Toxicol. XXXX, XXX, XXX–XXX

quickly to practically null within 2 h. Solutions affording stable CD spectra were obtained only through pretreatment of Aβ with a 1:1 mixture of HFIP and H_2O, in concurrence with previous reports by others.[25,26] Concentrations of Aβ at 50 μM also gave rise to CD spectra that showed rapid aggregation in less than 6 h.[27] Low concentrations of Aβ (1 μM) afforded ellipticities insufficient to afford CD spectra that could be interpreted. A concentration of 25 μM was therefore deemed to be optimum.

The solution of Aβ in PBS alone exhibited temporal changes in the CD spectrum with the presence of a single isodichroic point at ~203 nm, signifying two prominent conformations (Figure 2A). Analysis of the spectra by the CDpro software

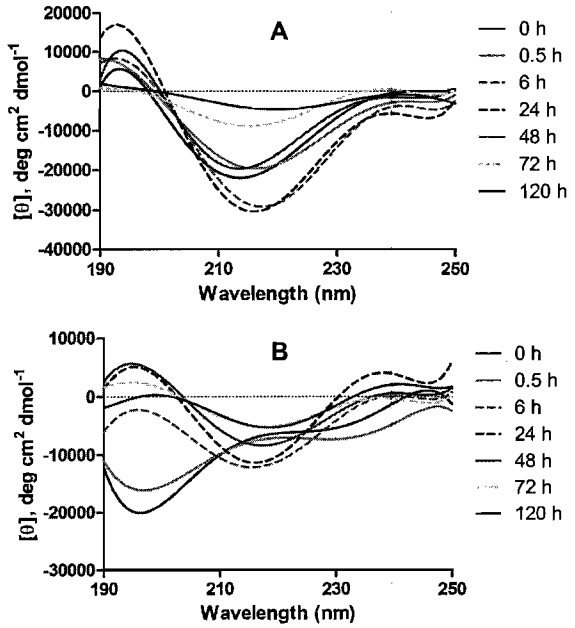

Figure 2. CD spectra of $A\beta_{1-42}$ (25 μM) in PBS (A) and in a 25 μM solution of DA in PBS (B), collected over 120 h at 37 °C. Curves are averaged over five scans. DA caused conformational changes indicative of accelerated aggregation.

package using the basis set = 10 indicated the presence of β-sheet and random-coil conformations with negligible helical content over the time intervals of 0–120 h. The time points of 72 and 120 h, however, afforded CD spectra with practically extinguished ellipticities and, therefore, patterns that should not be ascribed to definite secondary structures. Decreases in ellipticities at these time points are indicative of precipitation and, therefore, lower peptide concentration. Precipitation could have occurred throughout the course of this experiment; a fact that should be taken into account while calculating percentage contributions of secondary structures. Salomon et al.[4] have previously dealt with such a situation by calculating the percentage contribution of β-sheets according to the formula: β-sheet = $[(\theta_{195}/\theta_{218})_t/(\theta_{195}/\theta_{218})_{tmax}] \times 100$ (where t_{max} = time point at which the percentage β-sheet is maximum). This formula is based on the established fact that Aβ assumes a 100% β-sheet conformation before precipitation. Application of this line of reasoning to the data in plot A (Aβ alone; Figure 2) indicates that at time = 0, the contribution of β-sheet is 49%. This increases to 98% at 24 h, remaining steady until 48 h, after which interpretation of the CD curve becomes inconclusive due to precipitation of the peptide. It should be noted that although the peptide is fully in a β-sheet conformation at 24 h as well as 48 h, the latter case exhibits significantly reduced θ due to lower concentrations of the peptide still in solution.

The solution of Aβ in PBS containing 25 μM DA shows strikingly different CD spectra, both with respect to pattern and temporal changes. Between the time points of 0 and 48 h, an isodichroic point exists at ~209 nm, indicating interchange between two prominent conformations (Figure 2B). At 0 h and 30 min time points, the spectra indicate predominant random-coil conformation with minima at ~201 nm and the lack of minima either at ~208 or ~218 nm. At 6 h, the minimum at ~201 nm is lost in favor of a developing minimum at ~218 nm, indicating conversion of a predominantly random-coil-oriented conformation to a predominantly β-sheet conformation. This conversion is seemingly maximized at 24 h with a rise in |θ| values at both 195 and 218 nm, and the ratio $\theta_{195}/\theta_{218}$ is similar to that of Aβ in PBS alone at the corresponding time point. The absolute ellipticities, however, are less than twice in magnitude, suggesting precipitation to a higher degree. When a 25 μM solution of Aβ was incubated with a lower concentration of DA (1 μM), the CD spectra indicated that the peptide assumed predominantly β-sheet structure; however, aggregation was enhanced as the ellipticities decayed to near-zero at 48 h (Supporting Information, Figure S1).

Mass Spectrometric Analyses. A single-injection analysis of an aliquot of the Aβ peptide aged in a 25 μM solution of DA in PBS afforded two predominant masses (Supporting Information, Figure S2A). Deconvolution according to the ^{13}C isotope pattern indicated the presence of two pentacationic species. The species at the *m/z* group 903.3–904.3 averages to the root ion of 4519, which agrees with the calculated mass of pentaprotonated Aβ (4519). The species at the *m/z* group of

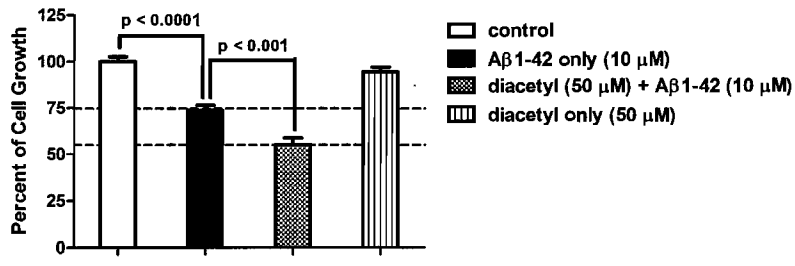

Figure 3. Cytotoxicity of $A\beta^{1-42}$ peptide in the presence of DA. SH-SY5Y cells were seeded in a 96-well plate and were exposed to DA alone (50 μM), $A\beta_{1-42}$ alone (10 μM), and a combination of DA (50 μM) and Aβ peptide (10 μM) for 24 h at 37 °C. After replacement of the $A\beta^{1-42}$ and/or DA-containing media with fresh media followed by 24 h of incubation, cell viability was determined by the MTT assay as described in the Materials and Methods. Data are expressed as the mean ± SEM of three independent experiments.

dx.doi.org/10.1021/tx3001016 | Chem. Res. Toxicol. XXXX, XXX, XXX–XXX

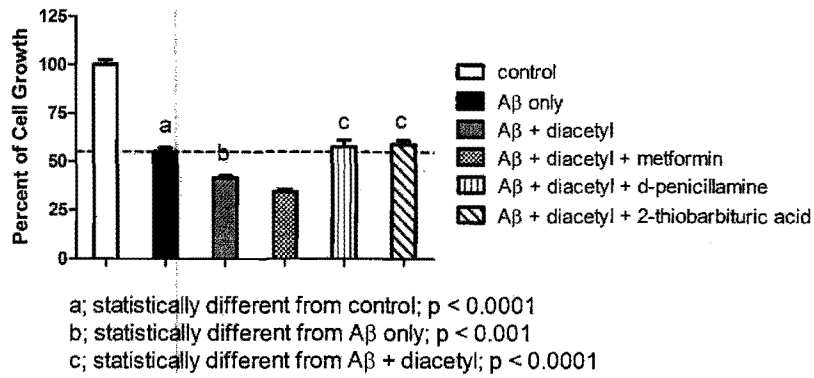

Figure 4. Protection of SH-SY5Y cells against DA-induced increase in $A\beta_{1-42}$ toxicity by carbonyl scavengers. DA was treated with metformin, 2-thiobarbituric acid, or D-penicillamine (1 mM) for 30 min, and the mixture was added to the cells. $A\beta^{1-42}$ was then added at a final concentration of 20 μM, and the mixture was incubated for 24 h. The media were replaced with fresh media (not containing DA or scavengers or $A\beta^{1-42}$), and the cytotoxicity was determined after 24 h through a standard MTT assay as described in the Materials and Methods.

920.5–921.5 averages to the root ion of 4605, which is the calculated mass of pentaprotonated Aβ + DA (4605). Limited Glu-C digestion afforded three significant fragments viz., $A\beta^{4-42}$, [DA + $A\beta^{4-42}$] and $A\beta^{12-42}$ (Supporting Information, Figure S2B). The presence of a [DA + $A\beta^{1-42}$] fragment and the absence of an adduct of $A\beta^{12-42}$ with DA, coupled with the ESI-MS analysis that indicates the formation of a 1:1 adduct between $A\beta^{1-42}$ and DA, suggests strongly that Arg^5 is the site of modification. This is consistent with previous findings that *N*-acetyl arginine forms a dihemiaminal adduct with DA and MEG forms an adduct with Arg^5 of $A\beta^{1-42}$.[28,29]

DA Potentiates $A\beta^{1-42}$ Cytotoxicity. $A\beta^{1-42}$ is cytotoxic to neuroblastoma cells in culture.[30] We determined the toxicity of $A\beta^{1-42}$ in SH-SY5Y, a human neuroblastoma cell line. Cell viability was calculated based on reduction of MTT as an indicator in a standard MTT assay setting. Exposure of SH-SY5Y cells to 10 μM of $A\beta^{1-42}$ resulted in a 26% cell death over an incubation period of 24 h (% cell viability: control, 99.9 ± 2.67; $A\beta^{1-42}$ alone, 73.7 ± 4.91; $p < 0.0001$; Figure 3). The addition of DA (50 μM) in addition to $A\beta^{1-42}$ (10 μM) increased cell death to 45% over control (% cell viability: $A\beta^{1-42}$ + DA, 54.9 ± 3.73; $P < 0.001$ as compared to $A\beta^{1-42}$ alone; Figure 3). DA (50 μM) alone, however, did not exhibit significant cytotoxicity under the incubation conditions employed in this assay (% cell viability: DA alone, 94.5 ± 4.50). DA concentrations in the low micromolar range that is known to be attained physiologically (2–5 μM) also resulted in statistically significant and measurable effect on $A\beta^{1-42}$ cytotoxicity (Supporting Information, Figure S3).

Classical Carbonyl Scavengers Protect against DA Induced $A\beta^{1-42}$ Toxicity in SH-SY5Y Cells. The addition of $A\beta^{1-42}$ at 20 μM concentration to SH-SY5Y cells resulted in 45% cell death (Figure 4). Admixture of DA (20 μM) with each of the carbonyl scavengers (1 mM) for 30 min followed by treatment of cells with the resulting mixture in the presence of $A\beta^{1-42}$ resulted in reversal of the DA effect. While metformin failed to reverse a DA-induced increase in $A\beta^{1-42}$ toxicity, D-penicillamine and 2-thiobarbituric acid afforded complete protection (% cell viability, $A\beta^{1-42}$ only, 55.2 ± 3.84; $A\beta^{1-42}$+DA, 41.5 ± 2.63; $A\beta^{1-42}$ + DA + metformin, 34.4 ± 2.35; $A\beta^{1-42}$ + DA + D-penicillamine, 57.7 ± 6.82; and $A\beta^{1-42}$ + DA + 2-thiobarbituric acid, 59.0 ± 4.10; Figure 4). When incubated concurrently with DA, only D-penicillamine was able to protect against DA-induced increases in $A\beta_{1-42}$ toxicity (data not shown).

DA Traverses through an in Vitro Blood–Brain Barrier Model. The transport of DA (100 μM) across a monolayer of MDR1-MDCK cells was determined over a period of 90 min (Figure 5A). The utility of MDR1-MDCK cells, MDCK-II

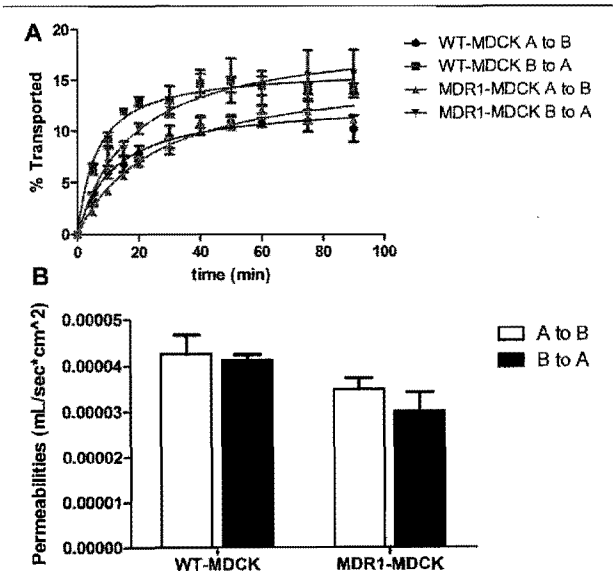

Figure 5. In vitro determination of BBB permeability to DA. MDCK cells, WT and MDR1 transfected, were seeded onto six-well Transwell inserts. The transport of DA from apical to basal direction and vice versa, along with its apparent permeability (P_{app}), was determined as described in the Materials and Methods.

transfected with the human MDR1 gene, has been widely accepted as an in vitro BBB model due to its ability to from tight junctions and expression of efflux transporters that are present at the BBB.[31] The percent transport and the apparent permeability of DA in MDR1-MDCK cells were compared to that in the WT MDCK cells. DA presented good permeability across the cell monolayer with A → B transport of 11.1 ± 0.18 and 10.2 ± 1.31% and B → A transport of 15.6 ± 2.37 and 14.2 ± 0.49% in MDR1-MDCK and WT MDCK cells, respectively, at the end of the experiment (i.e., 90 min). DA transport in both directions was found to be linear up to 15 min. To

dx.doi.org/10.1021/tx300101e | Chem. Res. Toxicol. XXXX, XXX, XXX–XXX

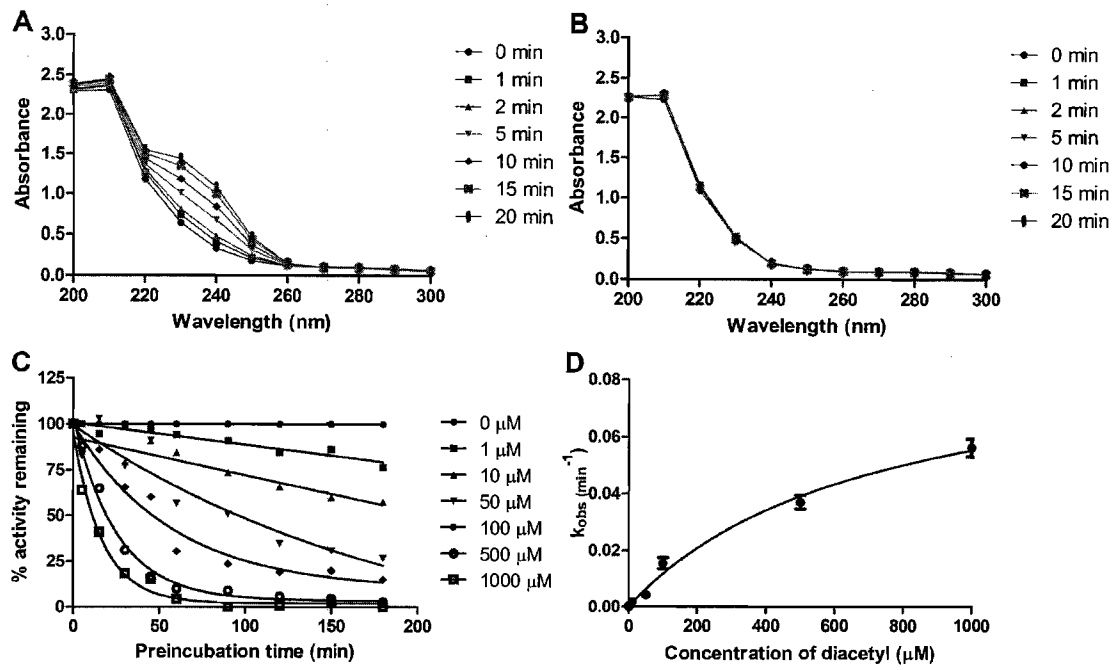

Figure 6. Glx-I enzyme kinetics assay. MEG (A) or DA (B) at various concentrations were incubated with GSH at 30 °C in phosphate buffer (0.05 M, pH 6.6) for 6 min to allow formation of the hemimercaptal, followed by the addition of yeast Glx-I. The enzyme reaction was monitored for absorption in the 200–300 nm wavelength range for 20 min. Absorbances were plotted against the wavelengths at various time points (0–20 min). Data shown here are representative of three independent experiments. (C) The residual activity of Glx-I was measured by percent of remaining enzymatic activity vs preincubation time in the presence of increasing concentrations of DA, showing time-dependent inactivation of Glx-I. (D) Plot of the observed rate of inactivation constants (k_{obs}) vs the concentration of DA, from which the kinetic parameters k_{inact} and K_I were determined as described in the Materials and Methods.

estimate the efficiency of DA transport and possible contribution of transporter-mediated permeation, an apparent permeability coefficient of DA was calculated. DA exhibited P_{app} of 3.56×10^{-5} and 4.35×10^{-5} mL/s cm^2 in the A → B direction and 3.13×10^{-5} and 4.31×10^{-5} mL/s cm^2 in the B → A direction of MDR1-MDCK and WT MDCK cells. The negative control, mannitol, under similar experimental conditions afforded a P_{app} of 5.31×10^{-7} mL/s cm^2 (Figure 5B). The absence of differences in P_{app} values of DA between the two directions suggests lack of active transport mechanism.

DA Is Not a Substrate of Glx-I. The enzymatic assay of Glx-I depends on the absorbance of the product formed by the reaction of Glx-I with the adduct of glutathione and MEG (the substrate), which is prominent at 240 nm. It was found that DA (5 mM) fails to cause an increase in absorbance at that wavelength when incubated with Glx-I and GSH (1 mM) at various time points (Figure 6B). Scanning the entire wavelength region 200–400 nm did not show a noticeable increase at any other wavelength. Because of absence of absorbance between 300–400 nm, the results are plotted from 200–300 nm (Figure 6A,B). MEG (5 mM), however, did lead to an increase in absorption at 240 nm (Figure 6A). Curiously, it was also found that the enzyme fails to form an adduct with MEG when it has previously been exposed to DA. Similar preincubations with MEG did not lead to inactivation of the enzyme reaction, indicating specificity of DA toward the Glx-I–MEG enzymatic reaction. Consistent with previous findings, DA was found to inactivate Glx-I in a time-dependent fashion. The rate constants for inactivation, k_{obs}, were dependent on the concentration of DA (pseudofirst order, Figure 6C,D). The rectangular hyperbola afforded by the plot of k_{obs} versus DA concentration implicates the formation of a reversible "E---I" complex prior to the actual kill step, that is, formation of a nondissociable E–I complex (Figure 6D). The rate constants of the kill step (K_{inact}; 0.094 min^{-1}) and the dissociation constant for the formation of the reversible E---I complex (K_I; 706 μM) were calculated from eq II (Materials and Methods).

DISCUSSION

Misfolding of the Aβ peptides is necessarily a pathological process. Their generation and breakdown in neuronal tissue constitute a delicate balance that ensures paucity of excessive amounts of free Aβ. RCS such as MEG that are naturally present in the brain represent a component of oxidative stress that affects this balance by stabilizing the peptidase-resistant β-sheet conformation of Aβ. Normally, such RCS are subject to detoxification mechanisms such as the glyoxalase pathway. Xenobiotic species such as DA that possess structure and reactivity similar to naturally occurring RCS, however, may not necessarily be detoxified by these mechanisms. This present study was conducted with two primary objectives: (1) to study whether DA affects Aβ chemistry, biophysics, and cytotoxicity and (2) to access the possibility of the effects of DA on Aβ being toxicologically significant. The research aims ultimately to begin a systematic probe into the chronic effects of DA on neuronal tissue.

ThT is a cationic benzothiazole dye that exhibits characteristic fluorescence changes upon association with β-pleated sheet structures derived from a variety of peptides and proteins.[32] It discriminates between unassociated and associated forms of the β-strand structures of Aβ, binding selectively to grooves between successive strands of β-pleated Aβ strands.[33] In

dx.doi.org/10.1021/tx3001016 | Chem. Res. Toxicol. XXXX, XXX, XXX–XXX

aqueous solutions, ThT fluoresces weakly with excitation maxima at 350 nm and emission maxima at 438 nm. Upon binding to Aβ or other β-pleated sheet structures, ThT fluoresces prominently with the wavelengths of maximal excitation and emission shifting bathochromatically to 440 and 490 nm, respectively. In this study, it was found that the solution of $A\beta_{1-42}$ shows a very slight increase over the first 24 h of incubation and a prominent increase in fluorescence intensity at the 48 h time point (Figure 1). This phenomenon corresponds to an initial lag phase consisting of slow, rate-limiting nucleation of the β-pleated structure followed by rapid oligomerization. A decrease in fluorescence of the solution after 48 h can be construed as precipitation of Aβ fibrils causing a lower amount of Aβ to be available for interaction with ThT. The latter phenomenon also indicates that the ThT-Aβ interaction is chemically specific and does not simply consist of the adsorption of ThT or its micelles[34] in water to a charged surface. DA-containing aqueous solutions of Aβ showed qualitatively similar, but temporally varied, behavior. ThT-induced fluorescence increased significantly over control over the first 24 h of incubation signifying truncation of the lag phase and accelerated nucleation. The fluorescence intensities at 48 h were also higher than the solution of Aβ not treated with DA, indicating a higher degree of β-pleated sheet formation.

The effect of DA treatment on the secondary structure of Aβ was immediately evident from CD studies of Aβ solutions in PBS (Figure 2). While Aβ alone assumed a mixture of β-sheet and random-coil (with the β-sheet being predominant) immediately after mixing with PBS, its dissolution into a 25 μM solution of DA in PBS afforded solutions whose CD spectra indicated predominant random-coil. While the spectra of Aβ alone in water did not change appreciably over 6 h, those of the DA-containing solution reflected a rapid conformational change from a random-coil to a β-strand. The population of β-strand reached values above 90% at 24 h in both of the solutions, but the ellipticity of the DA-containing solution was 2-fold lower, indicating a lesser amount of Aβ in solution. At 48 h, the ellipticity of the Aβ-only solution was 2-fold lower than that at 24 h, but ellipticity of the solution containing DA was practically extinguished. The conformational dynamics of Aβ in the DA-containing Aβ solution suggests that the DA–Aβ interaction drives the peptide in a conformational tumbling and aggregation pathway dissimilar from that when in solution alone. DA does seem to accelerate Aβ aggregation but through a different set of intermediate conformations. Ordinarily, Aβ in a random-coil conformation is nonamyloidogenic. The random-coil conformation induced by DA, however, is more prone to aggregation than the β-strand conformation of Aβ alone in solution. Lower (1 μM) concentrations of DA influenced $A\beta^{1-42}$, 25 μM, in a more subtle fashion. While the net conformational population of $A\beta^{1-42}$ remained unchanged, that is, remained predominantly in β-strands, all ellipticity was lost at 48 h (Supporting Information, Figure S1). It is arguable that the mechanism in this latter case is similar to that when equimolar concentrations of Aβ and DA are incubated together; however, the formation of Aβ–DA adducts are insufficient in number to influence overall CD over the wavelengths employed. Rather, the influence of the Aβ–DA adducts formed in low concentrations is reflected in the velocity of aggregation of the β-strands.

Mass spectrometric analysis of $A\beta^{1-42}$ aged in DA-containing PBS indicates covalent modification of the peptide. The prevalent species appears to be a 1:1 adduct of $A\beta^{1-42}$ and DA. Further probing through limited proteolysis and mass spectrometry indicates modification by DA at the N terminus with the fragment [$A\beta^{4-42}$ + DA] but not [$A\beta^{12-42}$ + DA] being prominently visible (Supporting Information, Figure S2). Arg^5 thus is very strongly implicated as a candidate for modification by DA. Others have reported a chemically stable adduct of *N*-acetyl arginine with DA, albeit not as part of a peptide sequence.[28] It is evident that the hydrophilic N terminus, which otherwise would promote solvation of $A\beta^{1-42}$ and in turn hinder aggregation, is rendered more hydrophobic by DA.

Solutions of Aβ and Aβ + DA that were utilized for cytotoxicity studies were prepared in a fashion identical to those for the CD spectral data collection (Figure 3 and Supporting Information, Figure S3). A solution of Aβ prepared by direct dissolution of the peptide in water was nontoxic toward SH-SY5Y cells. It is established from the CD spectral study that such a solution can be assumed to contain higher order/insoluble aggregates of Aβ, implying that under the incubation conditions, aggregated Aβ is not toxic toward SH-SY5Y cells. A solution prepared by pretreatment of Aβ with HFIP, on the other hand, was toxic over a period of 24 h, in turn implying that treatment of the cells with unaggregated or lower order/soluble aggregates of Aβ results in toxicity. This toxicity was magnified 2-fold with the inclusion of DA, suggesting that DA-induced Aβ aggregation is toxic either through acceleration of aggregation or through differing mechanisms of toxicity of the aggregates produced by the Aβ–DA interaction. In light of the rapid covalent adduct formation indicated by mass spectrometric analysis, it would seem that the adduct of DA and $A\beta^{1-42}$ is the species that is responsible for potentiating the cytotoxicity of $A\beta^{1-42}$. The prevention of DA-induced increase in $A\beta^{1-42}$ toxicity by carbonyl scavengers that sequester DA from $A\beta^{1-42}$ further supports this hypothesis (Figure 4).

The effects of DA on Aβ aggregation and cytotoxicity are toxicologically relevant only if DA reaches compartments that include neuronal tissue. Toward this end, the permeability of MDR1-MDCK cells to DA was examined (Figure 5). The MDR1-MDCK cell monolayer is an established model of the so-called "BBB", that is, endothelial cells that form a barrier between the CSF and other body compartments.[35] When this monolayer is placed between two fluids, the directionality of permeation (if any) is apparent from the differences between directional fluxes (i.e., the apparent permeability constant P_{app}). DA was found to permeate this barrier well, traversing at similar rates to the other compartment when placed in either side of the monolayer. This implies that an active transport mechanism is either absent or its contribution is not significant when compared to the sheer amount of DA that passively traverses the monolayer. The absence of differences in the percent transport and P_{app} values of DA in MDR1-transfected and WT MDCK cell serve to further illustrate the negligible effect of efflux transporters.

Normal physiological glycolysis produces significant amounts of dicarbonyl species such as MEG, to which DA bears close structural resemblance. The penetration of DA into CSF may be of no toxicological consequence if it is subject to metabolism by the glyoxalase pathway, which is the primary mode of MEG detoxification. Unfortunately, DA was not found to be a substrate for Glx-I, suggesting the possibility of significant residence of the former in the CSF (Figure 6B). Of greater concern is the observation that DA is an inhibitor of Glx-I

dx.doi.org/10.1021/tx3001016 | Chem. Res. Toxicol. XXXX, XXX, XXX–XXX

(Figure 6C,D). DA-induced Glx-I inhibition was time dependent and hence irreversible in nature. This inactivation has previously been recorded by others and has been attributed to the ability of DA to modify a crucial arginine in the Glx-I active site.[36] The mere presence of DA in the CSF would thus appear to hamper metabolism of MEG and other toxic dicarbonyl species, which in turn are established mediators of Aβ pathology.

Preliminary studies into the effect of classical carbonyl scavengers on DA-induced potentiation of Aβ cytotoxicity suggest that thiobarbituric acid, metformin, and D-penicillamine attenuate the effect of DA, with D-penicillamine (available OTC in the United States as Cuprimine) being the most effective in that regard.

DA is ubiquitous in the modern human diet and is present often as an added flavorant. Its utility resides in its concentration-dependent effects on taste perception, ranging from the "slippery" or "smooth" feel of beverages at lower concentration to the buttery flavor of popcorn at high concentrations. Whether toxic levels of DA are achieved in various body compartments upon mere (over)consumption of DA-containing food substances is an unanswered but an important question. A far trickier task is defining the toxicity referred to by the said "toxic levels" of DA. While the effects on the respiratory system upon inhalation of of DA have been studied, the chronic repurcussions of DA exposure on neuronal tissue are hitherto unknown. The present study establishes that DA alone strongly promotes amyloidogenesis at concentrations as low as 25 μM, with even lower concentrations of 1 μM having perceptible effects on the aggregation time of Aβ. A causative candidate event for this influence is the covalent modification of Aβ at Arg^5. We have now shown that DA potently enhances Aβ toxicity toward neuronal cells in culture at concentrations that is normally found in body compartments upon occupational exposure. DA is capable of permeating the BBB. It is additionally resistant to breakdown by glyoxalase. Its toxic effects could be magnified by its capacity to inhibit Glx-I, thus preventing detoxification of other amyloidogenesis-promoting dicarbonyls that are produced naturally in large quantities in the brain. Due caution must, however, be exercised while extrapolating the results of this study to phenomenon in the intact animal. Although the in vitro data in this study show toxicity of DA at concentrations actually recorded physiologically, extension of this toxicity in the in vivo environment is influenced by a plethora of factors ranging from transport across compartments to its possible metabolism of DA by dicarbonyl reductases. A study of the effects of such factors requires greatly expanded investigations employing animal models. To conclude, the multidisciplinary studies reported in this paper and their results establish a warrant for expanded studies of the neurological effects of DA exposure in the intact animal.

■ ASSOCIATED CONTENT

Supporting Information

Figures of CD spectra, mass spectrometric analysis, and DA-induced increases in the cytotoxicity of $A\beta_{1-42}$ peptide. This material is available free of charge via the Internet at http://pubs.acs.org.

■ AUTHOR INFORMATION

Corresponding Author

*E-mail: vince001@umn.edu.

Funding

This research study was supported by the Center for Drug Design (CDD) research endowment funds at the University of Minnesota, Minneapolis.

Notes

The authors declare no competing financial interest.

■ ACKNOWLEDGMENTS

Mass spectrometric analysis was conducted at the Department of Mass Spectrometry and Proteomics and the Department of Chemistry–Mass Spectrometry facilities, both at the University of Minnesota.

■ ABBREVIATIONS

DA, diacetyl; Aβ, amyloid β peptide; APP, amyloid precursor protein; AD, Alzheimer's disease; RCS, reactive carbonyl species; AGE, advanced glycation end products; CD, circular dichroism; MEG, methylglyoxal; Glx-I, glyoxalase I

■ REFERENCES

(1) Selkoe, D. J. (2000) Toward a comprehensive theory for Alzheimer's disease. Hypothesis: Alzheimer's disease is caused by the cerebral accumulation and cytotoxicity of amyloid beta-proteins. *Ann. N.Y. Acad. Sci. 924*, 17–25.

(2) Brown, M. S., Ye, J., Rawson, R. B., and Goldstein, J. L. (2000) Regulated intramembrane proteolysis: A control mechanism conserved from bacteria to humans. *Cell 100*, 391–398.

(3) Wang, J., Dickson, D. W., Trojanowski, J. Q., and Lee, V. M. (1999) The levels of soluble versus insoluble brain Abeta distinguish Alzheimer's disease from normal and pathologic aging. *Exp. Neurol. 158*, 328–337.

(4) Hu, X., Crick, S. L., Bu, G., Freiden, C., Pappu, R. V., and Lee, J. M. (2008) Amyloid seeds formed by cellular uptake, concentration, and aggregation of the amyloid-beta peptide. *Proc. Natl. Acad. Sci. U.S.A. 106*, 20324–20329.

(5) Brody, D. L., Magnoni, S., Schwetye, K. E., Spinner, M. L, Esparza, T. J., Stocchetti, N., Zipfel, G. J., and Holtzman, D. M. (2008) Amyloid-β dynamics correlate with neurological status in the injured human brain. *Science 321*, 1221–1224.

(6) Tennent, G. A., Lovat, L. B., and Pepys, M. B. (1995) Serum amyloid P component prevents proteolysis of the amyloid fibrils of Alzheimer disease and systemic amyloidosis. *Proc. Natl. Acad. Sci. U.S.A. 92*, 4299–4303.

(7) Haass, C., and Selkoe, D. J. (2007) Soluble protein oligomers in neurodegeneration: Lessons from the Alzheimer's amyloid β-peptide. *Nature Rev. Mol. Cell. Biol. 8*, 101–112.

(8) Heinitz, K., Beck, M., Schliebs, R., and Perez-Polo, J. R. (2006) Toxicity mediated by soluble oligomers of beta-amyloid (1–42) on cholinergic SN56.B5.G4 cells. *J. Neurochem. 98*, 1930–1945.

(9) Ramasamy, R., Yan, S. F., and Schmidt, A. M. (2006) Methylglyoxal comes of AGE. *Cell 124*, 258–260.

(10) Barrow, C. J., Uasuda, A., Kenny, P. T. M., and Zagorski, M. G. (1992) Solution conformations and aggregational proterties of synthetic amyloid β-peptides of Alzheimer's disease. *J. Mol. Biol. 225*, 1075–1093.

(11) Jarrett, J. T., and Lansbury, P. T. J. (1993) Seeding "one-dimensional" crystallization of amyloid: A pathologic mechanism in Alzheimer's disease and scrapie? *Cell 73*, 1055–1058.

(12) Tjernberg, L. O., Naslund, J., Lundqvist, F., Johansson, J., Karlstrom, A. R., Thyberg, J., Terenius, L., and Nordstedt, C. (1996) Arrest of beta-amyloid fibril formation by a pentapeptide ligand. *J. Biol. Chem. 271*, 8545–8548.

(13) Tjernberg, L. O., Callaway, D. J. E., Tjernberg, A., Hahne, S., Lilliehook, C., Terenius, L., Thyberg, J., and Nordstedt, C. (1999) A molecular model of Alzheimer Amyloid β- Peptide fibril formation. *J. Biol. Chem. 274* (18), 12619–12625.

(14) Vitek, M. P., Bhattacharya, K., Glendening, J. M., Stopa, E., Vlassara, H., Bucala, R., Manogue, K., and Cerami, A. (1994) Advanced glycation end products contribute to amyloidosis in Alzheimer disease. *Proc. Natl. Acad. Sci. U.S.A. 91*, 4766–4770.

(15) Dickerson, T. J., and Janda, K. D. (2003) Glycation of the amyloid β-protein by a nicotine metabolite: A fortituous chemical dynamic between smoking and Alzheimer's disease. *Proc. Natl. Acad. Sci. U.S.A. 100*, 8182–8187.

(16) Schrater, E. N. (2002) Popcorn worker's lung. *N. Engl. J. Med. 347*, 360–361.

(17) Kreiss, K., Gomaa, A., Kullman, G., Fedan, K., Simoes, E. J., and Enright, P. L. (2002) Clinical bronchiolitis obliterans in workers at a microwave-popcorn plant. *N. Engl. J. Med. 347*, 330–338.

(18) Martyny, J. W., Van Dyke, M. V., Arbuckle, S., Towle, M., and Rose, C. S. (2008) Diacetyl exposures in the flavor manufacturing industry. *J. Occup. Environ. Hyg. 5*, 679–688.

(19) LeVine, H, 3rd. (1993) Thioflavin T interaction with synthetic Alzheimer's disease beta-amyloid peptides: detection of amyloid aggregation in solution. *Protein Sci. 2*, 404–410.

(20) Barrow, C. J., Yasuda, A., Kenny, P. T., and Zagorski, M. G. (1992) Solution conformations and aggregational properties of synthetic amyloid beta-peptides of Alzheimer's disease. Analysis of circular dichroism spectra. *J. Mol. Biol. 225*, 1075–1093.

(21) Walker, J. M. *The Protein Protocols Handbook*; Humana Press: Totowa, NJ, 2002; pp 523–528.

(22) Revel, G., Nicolau-Pripis, L., Barbe, J.-C., and Bertrand, A. (2000) The detection of α-dicarbonyl compounds in wine by formation of quinoxaline derivatives. *J. Sci. Food. Agric. 80*, 102–108.

(23) Vince, R., and Wadd, W. B. (1969) Glyoxalase inhibitors as potential anticancer agents. *Biochem. Biophys. Res. Commun. 35*, 593–598.

(24) More, S. S., and Vince, R. (2009) Inhibition of glyoxalase-I: The first low-nanomolar tight-binding inhibitors. *J. Med. Chem. 52*, 4650–4656.

(25) Nichols, M. R., Moss, M. A., Reed, D. K., Cratic-McDaniel, S., Hoh, J. H., and Rosenberry, T. L. (2005) Amyloid-β protofibrils differ from amyloid-β aggregates induced in dilute hexafluoroisopropanol in stability and morphology. *J. Biol. Chem. 280*, 2471–2480.

(26) Wood, S. J., Maleeff, B., Hart, T., and Wetzel, R. (1996) Physical, morphological and functional differences between pH 5.8 and 7.4 aggregates of the Alzheimer's amyloid peptide Aβ. *J. Mol. Biol. 256*, 870–877.

(27) Salomon, A. R., Marcinowski, K. J., Friedland, R. P., and Zagorski, M. G. (1996) Nicotine inhibits amyloid formation by the β-peptide. *Biochemistry 35*, 13568–13578.

(28) Matthews, J. M., Watson, S. L., Snyder, R. W., Burgess, J. P., and Morgan, D. L. (2010) Reaction of the butter flavorant diacetyl (2,3-butanedione) with N-α-acetylarginine: A model for epitope formation with pulmonary proteins in the etiology of obliterative bronchiolitis. *J. Agric. Food. Chem. 58*, 12761–12768.

(29) Gomes, R., Sousa, S. M., Quintas, A., Cordeiro, C., Freire, A., Pereira, P., Martins, A., Monteiro, E., Barroso, E., and Ponces, F. A. (2005) Argpyrimidine, a methylglyxosal-derived advanced glycation end-product in familial amyloidotic polyneuropathy. *Biochem. J. 385*, 339–345.

(30) Li, Y. P., Bushnell, A. F., Lee, C. M., Perlmutter, L. S., and Wong, S. K. (1996) Beta-amyloid induces apoptosis in human-derived neurotypic SH-SYSY cells. *Brain Res. 738*, 196–204.

(31) Wang, Q., Rager, J. D., Weinstein, K., Kardos, P. S., Dobson, G. L., Li, J., and Hidalgo, I. J. (2005) Evaluation of the MDR-MDCK cell line as a permeability screen for the blood-brain barrier. *Int. J. Pharm. 288*, 349–359.

(32) Naiki, H., Higuchi, K., Hosokawa, M., and Takeda, T. (1989) Fluorometric determination of amyloid fibrils in vitro using the fluorescent dye, thioflavine T. *Anal. Biochem. 177*, 244–249.

(33) Krebs, M. R. H., Bromley, E. H. C., and Donald, A. M. (2005) The binding of thioflavin-T to amyloid fibrils:localisation and implications. *J. Struct. Biol. 149*, 30–37.

(34) Khurana, R., Coleman, C., Ionescu-Zanetti, C., Carter, S. A., Krishna, V., Grover, R. K., Roy, R., and Singh, S. (2005) Mechanism of thioflavin T binding to amyloid fibrils. *J. Struct. Biol. 151*, 229–238.

(35) Wang, Q., Rager, J. D., Weinstein, K., Kardos, P. S., Dobson, G. L., Li, J., and Hidalgo, I. J. (2005) Evaluation of the MDR-MDCK cell line as a permeability screen for the blood-brain barrier. *Int. J. Pharm. 288*, 349–359.

(36) Lupidi, G., Bollettini, M., Venardi, G., Marmochi, F., and Rotilio, G. (2001) Functional residues on the enzyme active site of glyoxalase I from bovine brain. *Prep. Biochem. Biotechnol. 31*, 317–329.

dx.doi.org/10.1021/tx3001016 | *Chem. Res. Toxicol.* XXXX, XXX, XXX–XXX